Electronic Supplementary Information

for

Dimpled SiO$_2$@γ-Fe$_2$O$_3$ nanocomposites – fabrication and use for arsenic adsorption in aqueous medium

Saruta Deeprasert,[a,b] Lilin Wang,[a,b] Konstantinos Simeonidis,[c] Nguyen Thi Kim Thanh,[a,b,*] Etienne Duguet,[d,*] Stefanos Mourdikoudis,[a,b,*]

[a] Biophysics Group, Department of Physics and Astronomy, University College London, London, WC1E 6BT, UK

[b] UCL Healthcare Biomagnetic and Nanomaterials Laboratories, 21 Albemarle Street, London W1S 4BS, UK

[c] Department of Physics, Aristotle University of Thessaloniki, 54124 Thessaloniki, Greece

[d] Univ. Bordeaux, CNRS, Bordeaux INP, ICMCB, UMR 5026, F-33600 Pessac, France
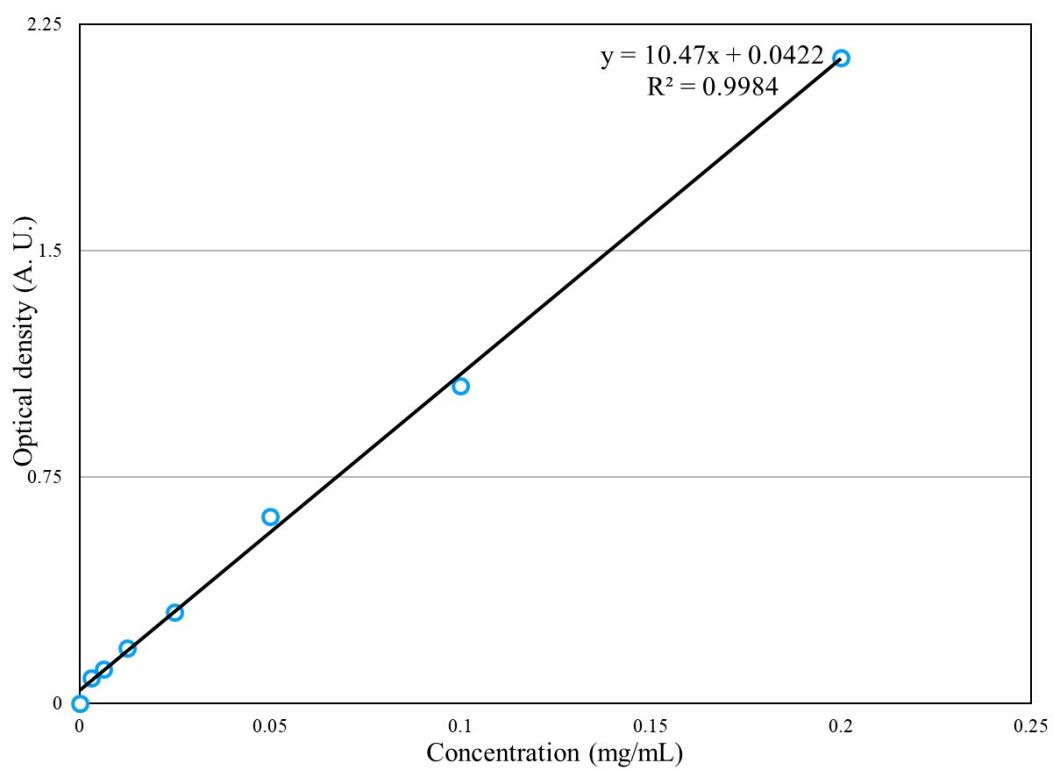
$$y = 10.47x + 0.0422$$
$$R^2 = 0.9984$$

Fig. S1 Calibration curve created by UV-Vis measurements of Fe-containing samples with known concentration.

a)

Size Distribution by Intensity

b)

Size Distribution by Intensity
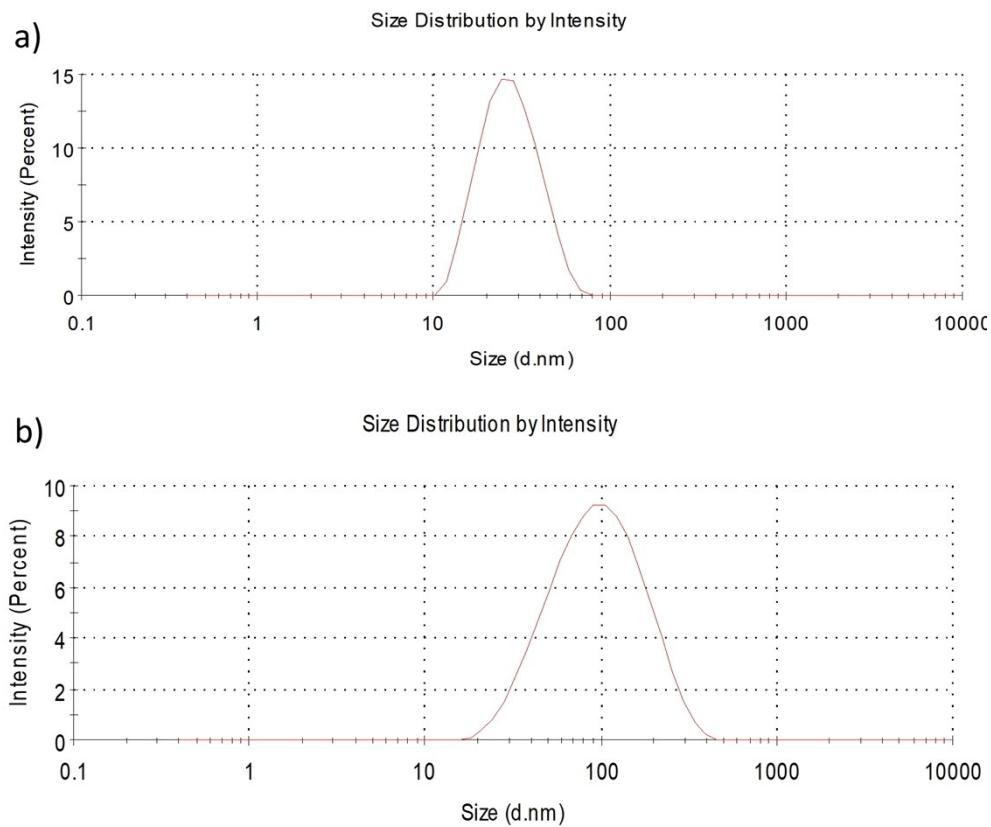
Fig. S2 DLS measurements for citrate-capped (a) and uncapped γ-Fe$_2$O$_3$ NFs (b).

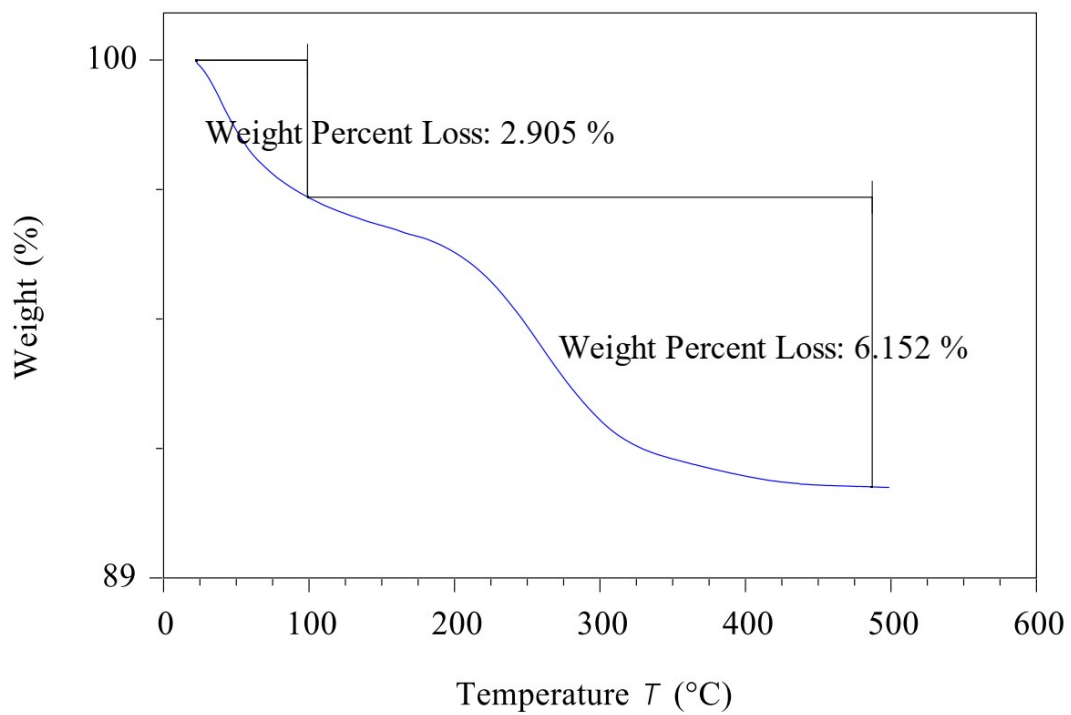Weight Percent Loss: 2.905 %

Weight Percent Loss: 6.152 %

Fig. S3 Thermogravimetric analysis of maghemite NFs.
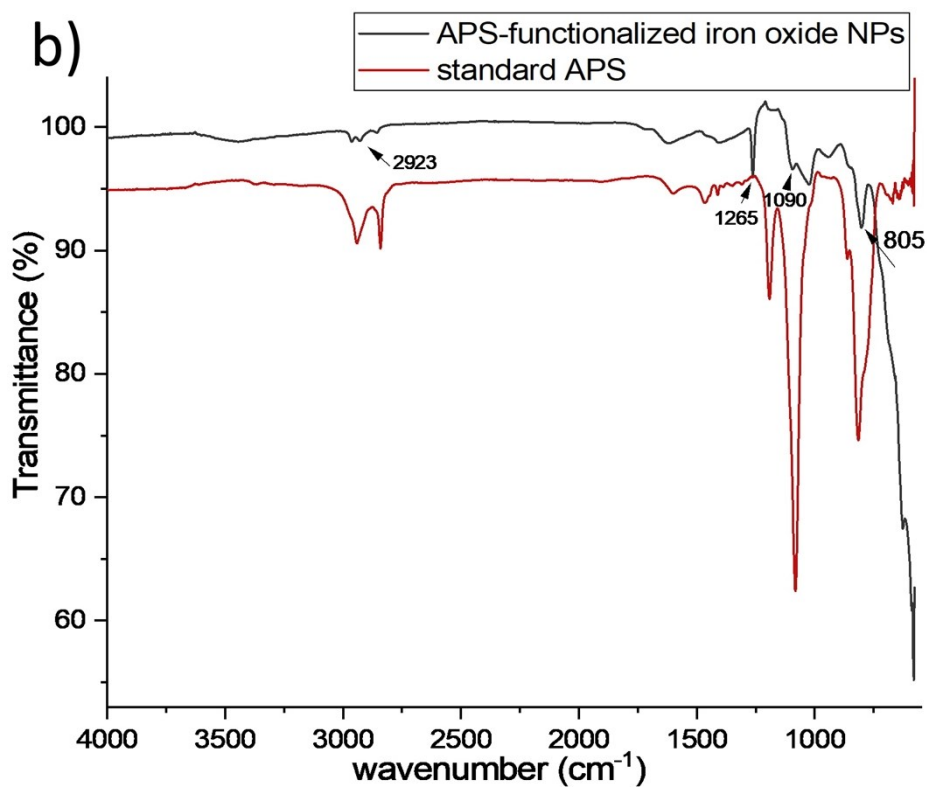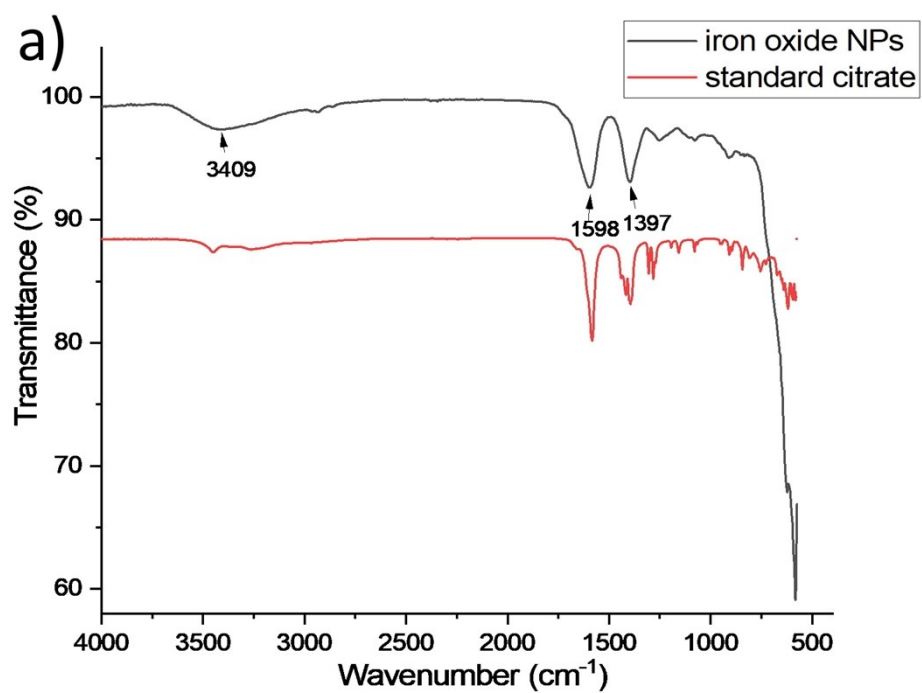
Fig. S4 FTIR spectra of: a standard citrate sample and of the pre-synthesized iron oxide NPs (a), APS molecule and APS-modified iron oxide NPs (b).
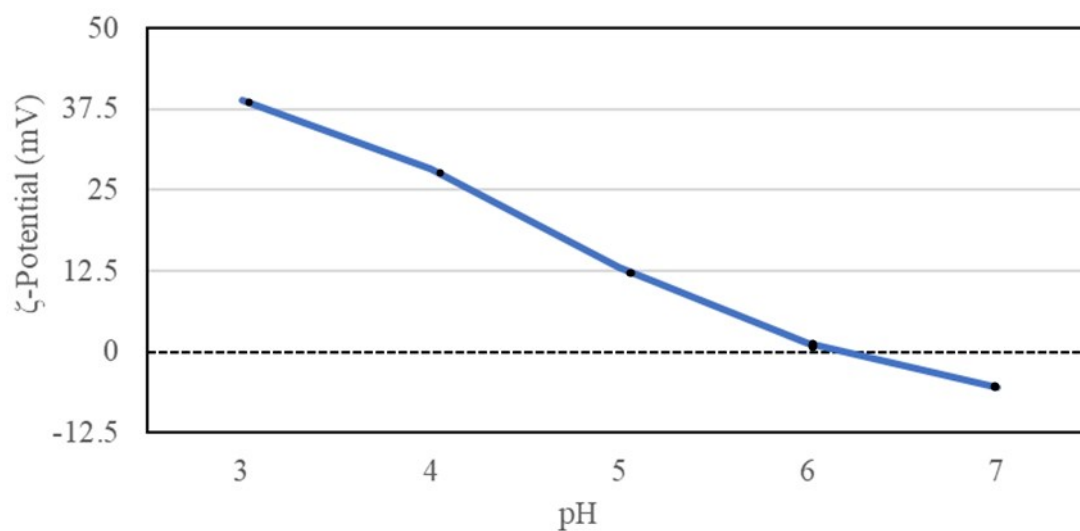
Fig. S5 ζ-potential measurements of the initial iron oxide NPs in a range of different pH values.
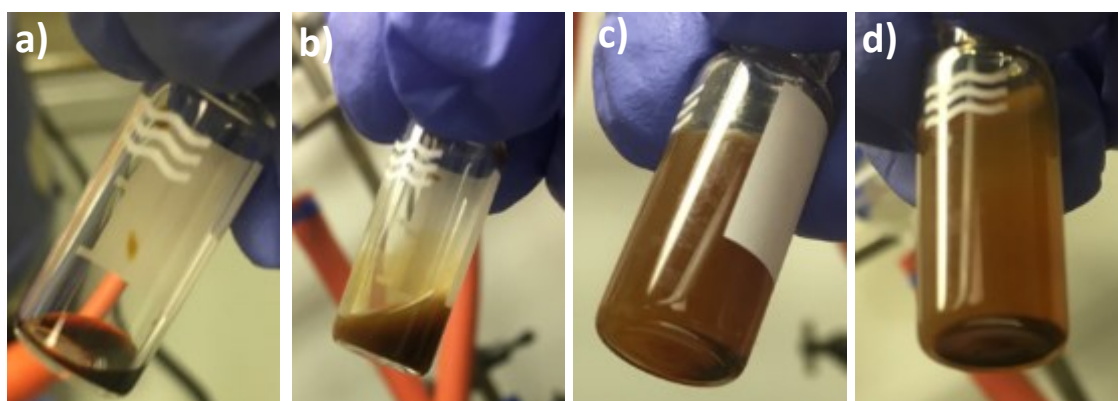

Fig. S6 Photographs of the dispersion of pre-treatment iron oxide NPs: a) no nitric acid added, b) 0.5 ml of 0.1 M nitric acid added, c) 1 ml nitric of 0.1 M nitric acid and d) 1.5 ml of 0.1 M nitric acid added.
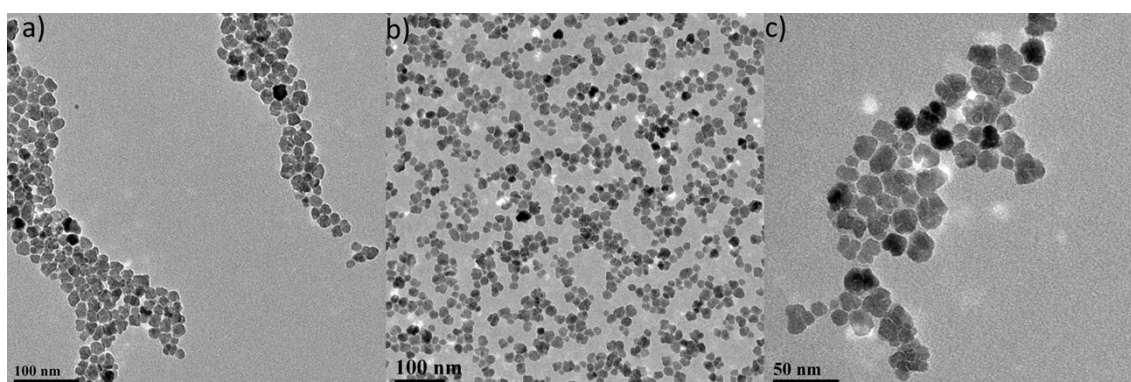

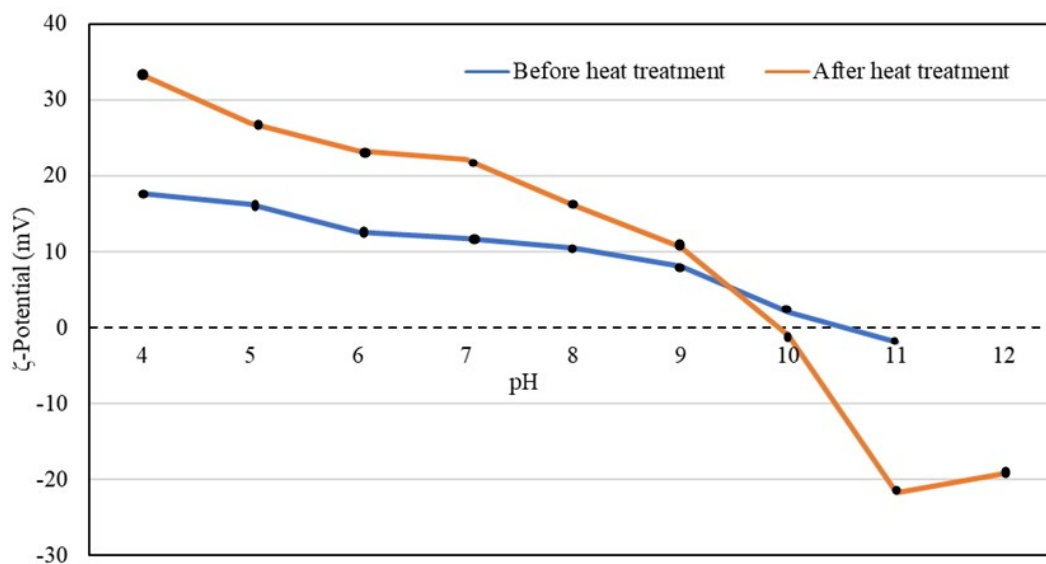**Fig. S7** TEM images of APS-modified iron oxide nanoparticles

Fig. S8 ζ-potential measurement of APS-modified iron oxide NPs before and after heat treatment at 110 °C

Table S1: FTIR absorption frequencies of standard APS[S1]

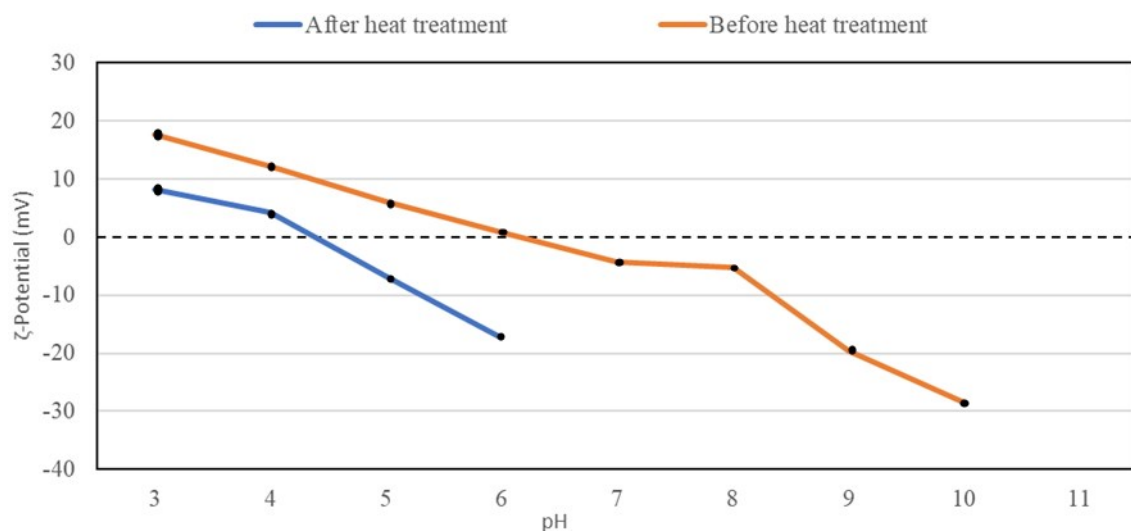| Wavenumber (cm^{-1})	Intensity	Assignments
816	Strong	Si-O-CH$_3$ stretching
1083	Very Strong	Si-O-C stretching
1118	Strong	O-CH$_3$ rocking
1455	Medium	CH$_2$ shearing
1588	Weak	NH shearing
2842	Strong	O-CH$_3$ stretching
2930	Strong	CH$_2$ stretching

Fig. S9 ζ-potential measurements of the carboxylic acid-modified iron oxide nanoparticles before and after heat treatment.
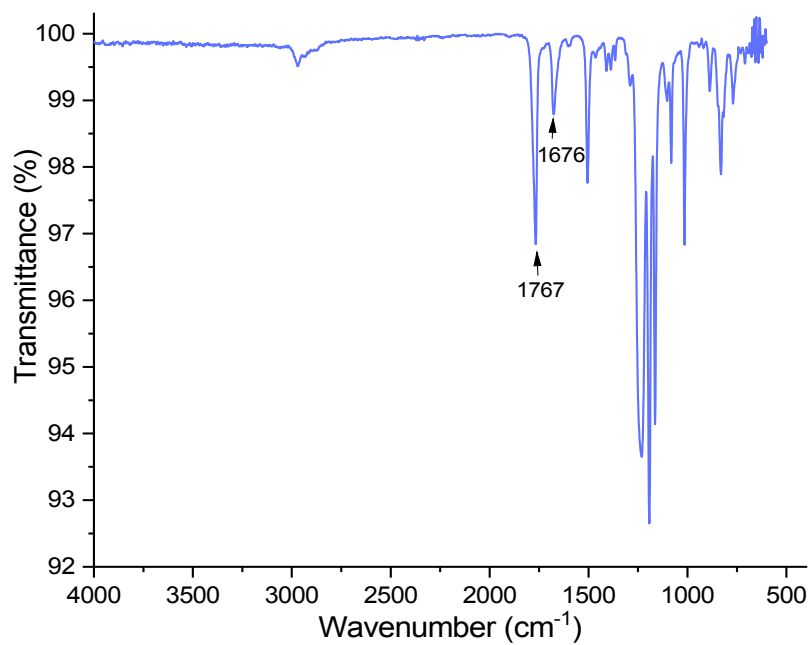

Fig. S10 FTIR spectrum of carboxylic acid-modified iron oxide nanoparticles
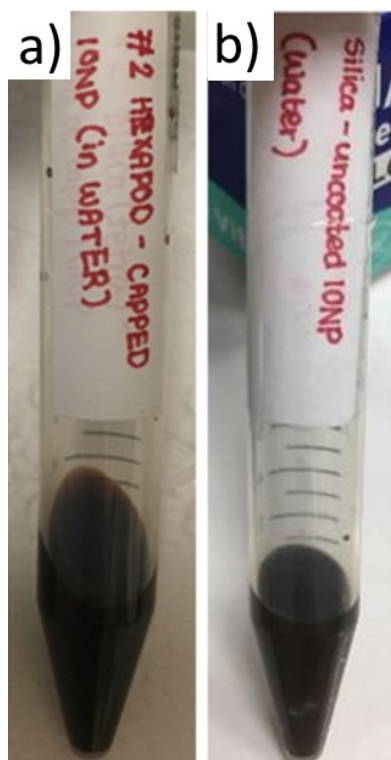
Fig. S11 Visual images of the colloidal dispersion of nanocomposites consisting of silica dimples and citrate-capped iron oxide NFs a) and uncapped iron oxide NFs (b). The latter sample was used for As removal
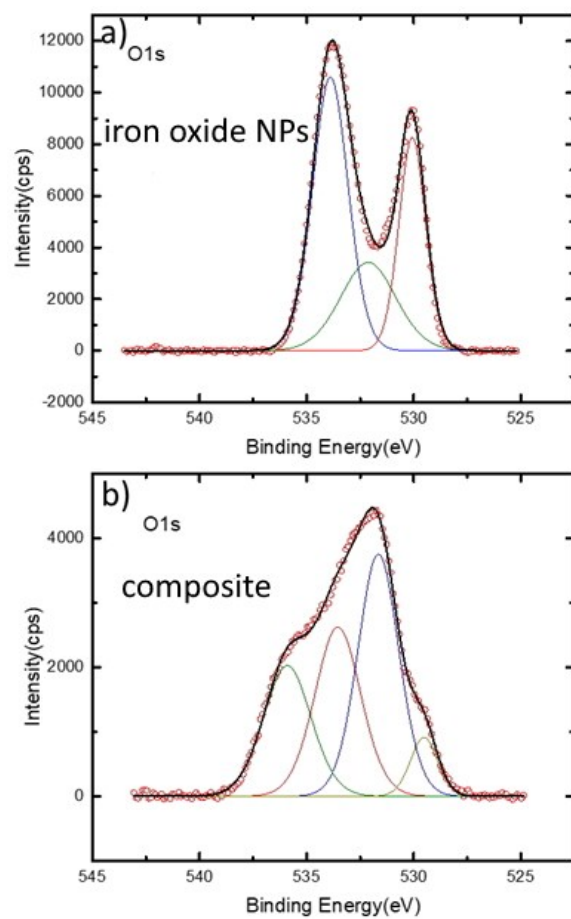
Fig. S12 High-resolution XPS spectra at the O1s: a) iron oxide NPs, b) silica dimples@iron oxide NPs
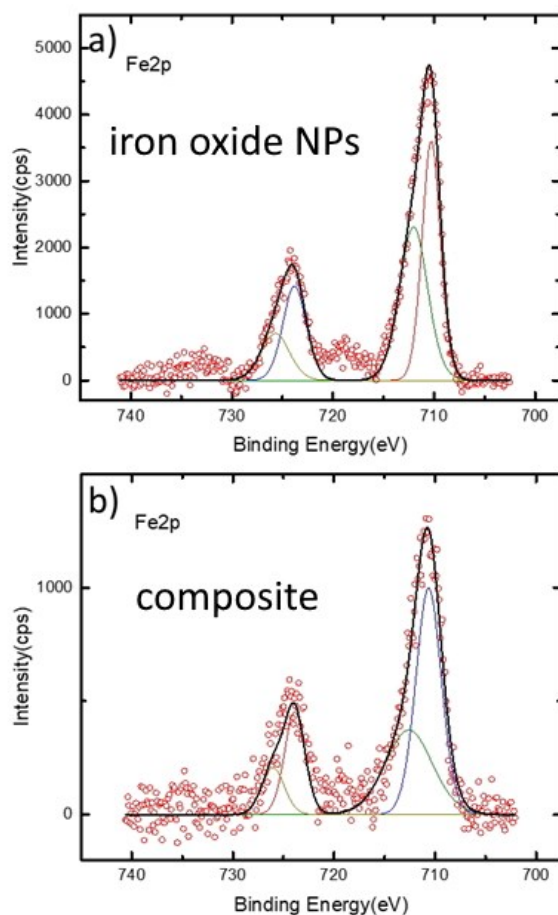
Fig. S13 High-resolution XPS spectra at the Fe2p a) iron oxide NPs, b) SiO$_2$ dimples@iron oxide NPs

Table S2: As-to-Fe mass ratio determined by XPS for various As(V) concentrations and acidities for silica dimples@iron oxide NPs

pH	As(V) concentration (mg/L)	As/Fe
6	1	0.011
6	5	0.028
6	10	0.052
6	20	0.097
8	10	0.033
10	10	0.024

(S1)   S. Mornet, J. Portier and E. Duguet, *J. Magn. Magn. Mater.* 2005, **293**, 127

References